What Sets the Lifetime of Thin Films of Binary Mixtures?

A. Choudhury,[1,2] L. Duchemin,[1] F. Lequeux,[2] and L. Talini[3]

[1] *PMMH, CNRS, ESPCI Paris, Université PSL, Sorbonne Université, Université de Paris, F-75005, Paris, France*
[2] *CNRS, Sciences et Ingénierie de la Matière Molle, ESPCI Paris, Université PSL, Sorbonne Université, 75005 Paris, France*
[3] *CNRS, Surface du Verre et Interfaces, Saint-Gobain, 93300 Aubervilliers, France*

(Dated: February 11, 2024)

In binary mixtures, the lifetimes of surface bubbles can be five orders of magnitude longer than those in pure liquids because of slightly different compositions of the bulk and the surfaces, leading to a thickness-dependent surface tension of thin films. Taking profit of the resulting simple surface rheology, we derive the equations describing the thickness, flow velocity and surface tension of a single liquid film. Numerical resolution shows that, after a first step of tension equilibration, a parabolic flow with mobile interfaces is associated with film pinching in a further drainage step. Our model paves the way for a better understanding of the rupture dynamics of liquid films.

The lifetimes of foams and surface bubbles are primarily governed by the drainage and rupture processes of the thin liquid films surrounding bubbles. These processes are influenced by various intricate - and sometimes difficult to control - factors, including contamination [1], physicochemical properties of added surfactants [2], evaporation [3] and history of thin film formation [4, 5], which may induce variations in lifetimes over several orders of magnitude. In the presence of surface active species, a comprehensive description of the drainage of thin films is made difficult even in controlled conditions, particularly because of the coupling of flow with concentration field of species. Further complexity arises from the timescales of surface and bulk exchanges of surfactant, which can be comparable to the drainage time [6]. Generally, surface rheology is accounted for by using a velocity boundary condition corresponding to an immobile interface with air, leading to a Poiseuille flow within the film. Although this is a fair assumption leading to a simple lubrication equation for film thickness, it ignores the evolution of surface tension field in the liquid film.

Recently, the foaming of oil mixtures has attracted renewed interest [7, 8]. The relatively stable foams that can form in these mixtures without any surfactant have been evidenced decades ago [9], and are currently observed in many processes of the oil industry, for example car tank filling and crude oil extraction, or in the food industry, for instance, in frying oils. Anti-foaming molecules are then often required to increase efficiency [10]. In the absence of evaporation, it has been shown that the enhanced lifetimes of thin films in mixtures stem from slight differences between the bulk and surface concentrations of different species, leading to thickness-dependent surface tensions of thin films [11, 12]. Since the diffusion times of small molecules are very short, bulk and interfaces can be considered to be in thermodyamical equilibrium (the time for a molecule to travel across the thickness of a film is $h^2/D \sim 1$ ms for a 1 μm thick film). Thus, the surface rheology of mixtures reduces to Gibb's elasticity [13]. In addition, the disjoining pressure is purely attractive, therefore binary oil mixtures constitute much simpler systems than surfactant solutions to study the drainage mechanisms of liquid films.

Recent insight has been offered on the process of film drainage and rupture, which may be divided into three stages [1, 12, 14]. The first stage comprises of the thin film formation; from spherical surfaces to locally flat surfaces. In case of binary mixtures, this shape can be described using a mechanism of equilibration of film tension by a balance between surface tension gradient and the pressure gradient due to Laplace pressure difference [12]. This equilibrium shape is reached in a few milliseconds. Naturally, a second stage dynamics ensues, relaxing the pressure gradient and causing a more complicated film drainage scenario. The relaxation causes the film to drain via dimpled (marginal) pinching, as described in soap films [14, 15]. At one point, the film becomes so thin that a third stage of van der Waals attraction becomes effective and causes spontaneous rupture [16, 17]. The film lifetime is thus mostly determined by the second stage of film drainage when a pinched part reaches a critical thickness, which is much longer than the initial viscous stretching phase and the final spontaneous rupture due to van der Waals interactions. Existing models developed for pinching of films of surfactant solutions are based on immobile interfaces [4, 15, 16], and they cannot predict quantitative lifetimes observed in thin films of binary mixtures [12].

In this letter, we formulate a robust model describing the first two stages of marginal pinching of films of binary mixtures. Our model presented here does not impose immobile interfaces a priori, and the pinching dynamics is described by three 1D coupled evolution equations for film thickness h, mean flow velocity $\overline{u}$ and surface tension γ. In the past, models for films with surfactant-like effects describing parabolic flow with mobile interfaces have been developed [17, 18]. However, they have a general description for surface tension evolution in terms of surfactant concentration with empirical Marangoni parameters. In contrast, we obtain an evolution equation

for surface tension, here in the context of binary mixtures, using thermodynamic principles of ideal solution theory. As a result, the parameters defining the surface tension gradient are fully determined by the chosen bulk concentration of the mixture species with lower surface tension. In general, if physicochemical relations between surface tension and the source field of surface elasticity are known (surface excess is well defined), our derivation approach can be readily used to derive the evolution equation of surface tension in other systems like sparse surfactants [1] and electrolyte solutions [17], governed by linear variation of surface tension.

To test our model, we take a simple geometry of ligament bounded within a characteristic length $\mathcal{L}$, and thickness at the boundaries $\mathcal{H}$. This configuration is close to a film in a Scheludko cell. Initially, a flat-film profile of thickness, $h_i = 500$ nm is prescribed in the middle (spanning a length of $\mathcal{L}/2$) conjoined to a Plateau border of radius, $R_b = 1$ mm. This is described in details in [19]. The estimations are taken from experimental values reported in [12]. We model the ensuing drainage dynamics using conservative laws for mass, momentum and mixture species. In the following, we use subscripts (x, t) to denote derivatives (∂_x, ∂_t) in the equations. The horizontal velocity is written as $u = \bar{u} + u_{Po}(z^2/h^2 - 1/12) + O(z^4)$. The average velocity $\bar{u}$ is responsible for the shape evolution of the film, and the velocity u_{Po} - which is proportional to the square root of the variance of the velocity over the vertical direction - is responsible only for the relative motion of the surface and the bulk and thus for the non-uniform advection of species. The mass conservation of the film writes as:

$$D_t h = -h\overline{u}_x, \tag{1}$$

where the material derivative $D_t = \partial_t + \overline{u}\partial_x \sim \partial_t$ since inertia is negligible. The conservation of momentum in a thin liquid film along with interfacial stress conditions can be effectively reduced to an evolution equation for $\overline{u}$ (see Refs. [19] & [20] for details):

$$D_t\overline{u} = \frac{1}{\rho h}\left(2\gamma_x + \frac{\gamma_0 h h_{xxx}}{2}\right) + \frac{\mu}{\rho}\frac{(4h\overline{u}_x)_x}{h}. \tag{2}$$

Here, ρ, μ are the density and viscosity of the liquid mixture respectively and γ_0 is the reference surface tension of the liquid mixture at infinite film thickness. The first term in eq. (2) can be identified as the gradient of film tension C at the leading order in h_x. More precisely, in the limit of small curvatures and slopes, it can be written as $C = \gamma\left(2 - h_x^2/4 + hh_{xx}/2\right)$, as obtained previously in Ref. [12]. The last term originates from the classical Trouton viscosity which is the ratio of elongational to shear viscosity for planar Newtonian viscous flows appropriate for thin films [21].

Lastly, we need to introduce the relation between species concentration and surface tension, to couple the flow with the surface tension gradient. As discussed in [11, 12], under stretching, a film ligament of binary mixture experiences an increase of surface tension. This increase also corresponds to the Gibbs elastic modulus and is given by $\alpha\gamma_0/h$, where α is a length related to the concentration differences between bulk and interfaces. These differences are modeled in the framework of the thermodynamics of ideal solutions [22], and we assume similar molar volume and surface of both constituents for the sake of simplicity. The resulting length α exhibits a maximum value of the order of 10^{-1} nm, is a function of the species volume fraction, and vanishes for pure liquids. Since the surface tension varies weakly during the whole pinching process (typically differences of $10^{-3}\gamma_0$ are involved in these phenomena [11]), we linearly expand the surface tension of the film according to δ, the thickness of the interface (about 1 nm), and the global film composition $X = (hc + 2\Gamma\delta)/(h + 2\delta)$ around the initial uniform composition X_0. Here Γ and c are respectively the surface and volume molar fractions of the species with the lower surface tension. We can thus write the surface tension as: $\gamma = \gamma_0\,(1 + \alpha/h - \beta(X - X_0))$. The term $\alpha\gamma_0/h$ is the Gibbs elastic modulus of the film whereas β is a positive dimensionless solutal Marangoni coefficient. If the composition at the interface Γ and the one in the bulk c are different, the parabolic flow u_{Po} contribution to the velocity field will advect differently bulk and interfacial species and the concentration field X will be modified with a flux proportional to $u_{Po}h(\Gamma - c)$. In addition, the Marangoni stress controls the velocity gradient at the interface and thus u_{Po} is also found to be proportional to γ_x. Thus the parabolic velocity field leads to the evolution of X through a term $(\Gamma - c)(h\gamma_x)_x$. Finally, the relation between the concentration X, the height h and the interfacial tension γ allows to close the system of equations leading to the evolution equation for γ. It can be obtained by the time derivative of the expression for interfacial tension in terms of δ/h and $X - X_0$ written above and using the conservation of species. As detailed in [19], it is written as:

$$D_t\gamma = \delta\gamma_0\beta(\Gamma_0 - c_0)\left(2\frac{\overline{u}_x}{h} + \frac{1}{3\mu}\frac{(\gamma_x h)_x}{h}\right), \tag{3}$$

where c_0, Γ_0 are the reference bulk and surface concentrations (in molar fractions) of the binary mixture respectively. Note that α is explicitly written as $\alpha = \delta\beta(\Gamma_0 - c_0)$. The first term in the r.h.s. account for the Gibbs' elasticity, while the second term describe the effect of the Marangoni stress. The equations (1), (2) and (3) constitute a system of coupled evolution equations necessary to describe the drainage inside a thin film of binary mixture. This system of equations is solved, with appropriate initial and boundary conditions [19], using a second-order finite difference scheme, with adaptive time-step [23]. In the limit of vanishing surface tension gradient for pure fluids because in that case $\Gamma_0 = c_0$, eq.

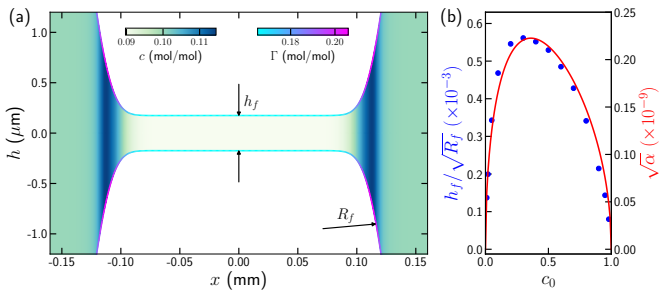

FIG. 1. (a) Tension equilibrated film profile and corresponding surface (Γ) and bulk (c) molar fraction distribution for a thin-film of octane-toluene mixture at $t \sim 5 \times 10^{-3}$ s. (b) Variation of tension equilibrated film thickness, h_f [blue] and the Gibbs parameter, $\alpha = \delta\beta(\Gamma_0 - c_0)$ [red] as a function of the reference bulk molar fraction of octane, $c_0 = [0.01 - 0.98]$.

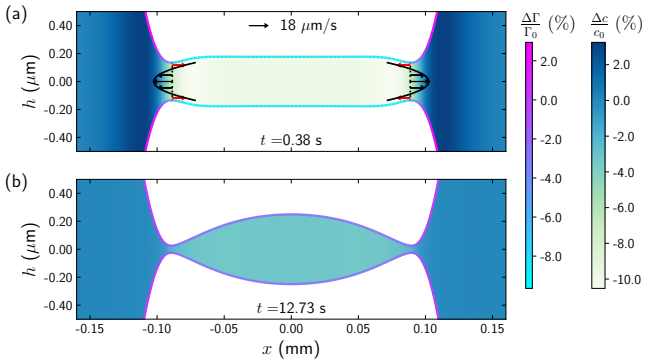

FIG. 2. Evolution of marginal pinching in octane-toluene mixture: (a) formation of marginal pinch; (b) thickness of the film reaches h_c. The arrows denote the evolved velocity in the film, enveloped by the velocity magnitude at the pinch locations. $\Delta\Gamma = \Gamma - \Gamma_0$ and $\Delta c = c - c_0$, where $\Gamma_0 = 0.1856$ and $c_0 = 0.1$ are reference quantities for surface and bulk molar fraction (for octane) respectively.

(3) becomes redundant and eqs. (1) and (2) reduce to a system of equations describing drainage via plug-flow governed only by viscous stretching [18, 24]. The evolution of the film from an initially prescribed flat interface to a flat profile equilibrated in tension and subsequently to the dimpled shape film thinning is predicted by our reduced-order numerical model and showcased in a supplemental video [19].

The initial tension relaxation process lasts an inertio-capillary time, $T_c \sim \sqrt{\rho\mathcal{L}^4/\gamma_0\mathcal{H}}$ [1]. This early dynamics ensures mechanical equilibrium in film tension C. Fig. 1 (a) shows a typical profile obtained from our model simulation due to an initial stage of tension equilibration. At this moment, the film thickness, h_f and radius at the Plateau border, R_f is plotted in fig. 1 (b) for the range of mixture concentrations. It satisfactorily matches the analytical scaling: $h_f \sim \sqrt{\alpha R_f}$, previously derived in [12]. When a Marangoni stress exists, the drainage time becomes much larger giving a film pinching lifetime, $T_p \gg T_c$ and eq. (3) then dominates the film evolution.

It is important to note that the set of eqs. (1) - (3) is different from the case of an immobile interface assumption used in Refs. [4, 15, 16]. In contrast to the classical approach of prescribing immobile interfaces and excluding plug-flow [15], our model describes the leading order plug-flow in the film evolution (eqs. (1), (2)) that equilibrates the film tension. However the pressure is not equilibrated and generates a slow Poiseuille flow. This Poiseuille flow advects differently species at the interfaces and in the bulk, leading to a slow modification of the concentration and thus to the surface tension (eq. (3)). The surface tension evolution in turn modifies the tension equilibrium. Indeed, the parabolic part contribution to the viscous stress is of $O(h^2)$ compared to the plug flow that relaxes the tension gradient, and is apparently negligible. However, it is subtly included in the derivation of eq. (2) and is the source of non-uniform advection of species and thus of the Marangoni effect, that leads eventually to pinching.

Fig. 2 shows snapshots for the initial (a) and the final (b) scenarios of the dimple drainage mechanism governed by Poiseuille flow for a typical binary mixture of octane-toluene. Since the surface tension varies inversely with global concentration and with the film thickness, the central part of the film has a higher surface tension. This translates to a Marangoni stress $\sim \partial_x\gamma$ in the negative direction with respect to capillary drainage. Thus, throughout the film evolution, a Marangoni flux opposes the capillary flow, spontaneously maintaining a parabolic flow profile in the bulk, but with a non zero velocity at the interfaces.

The driving mechanism for film evolution is the surface tension difference via the second term in the r.h.s of eq. (3). The overall film evolution dynamics thus work towards minimising this difference (plotted as $\Delta\gamma/\gamma_0$ in fig. 3(a)). Since the pressure gradient is concomitant with the surface tension gradient (through the balance of film tension shown in fig. 3(d)), it is corollary to say either of the two gradients is minimised during the film evolution. Fig. 3(b) shows the model predictions of the mean (plug-flow) and parabolic (Poiseuille flow) velocities, which asymptotically approach to zero during the remaining process of dimpled drainage. The evolution of curvature at the pinch location, $\kappa = h_{xx}/2$ is shown in Fig. 3(c). Contrary to the earlier study of [15], where they predict a scaling for κ, we do not observe any scaling for the same, and it essentially remains constant throughout the pinched draining stage. Note that, in the absence of van-der Waals' attractive forces, there is no mechanism for destabilisation and rupture in our model. All the physical quantities like $\Delta\gamma$, h_{min} and $\overline{u}$ - approach zero asymptotically. Henceforth, to estimate the film life-

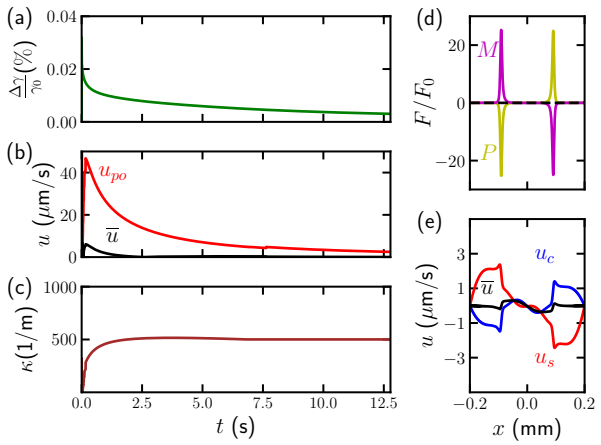

FIG. 3. Pinching dynamics of a thin film of Octane-Toluene mixture: evolution of (a) surface tension difference $\Delta\gamma = \gamma_{max} - \gamma_{min}$ across the Plateau border; (b) velocities at the pinch location: mean (plug-flow) velocity $\overline{u}$ and parabolic (Poiseuille flow) velocity $u_{po} = u^{(2)}h_{min}^2$; (c) maximum curvature, κ at the pinch location. Across the film length at $t = 12.73$ s: (d) dimensionless force/mass due to Laplace pressure gradient (P) and Marangoni stress (M) where $F_0 = 1.73 \times 10^3$ N/Kg. (e) spatial variation of $\overline{u}$, surface velocity u_s, centerline velocity u_c.

time, we choose a cutoff film thickness, $h_c \sim 50$ nm when it is safe to assume that van der Waals force causes spontaneous rupture. A precise discussion of the role of Van der Waals force shows that it marginally modifies the pinching dynamics and that the assumption of rupture occurring when $h = h_c$ is correct [16]. Fig. 3(e) shows the surface velocity profile across the film length. It is always opposite compared to the capillary drainage velocity ($\overline{u}$ or u_{Po}) during the entire duration of the film evolution.

We now dig deeper into the various mechanisms at play during the film thinning process showcased in fig. 4 and in the supplemental video [19]. At the very shortest timescale, the film tension is equilibrated as explained previously. Since our initial condition is out of this force equilibrium, a quick transient phase can be observed initially. Next, a plug-flow develops causing a *pure stretching* mode which governs the process of equilibration of the film tension, i.e., a surface tension gradient develops which balances the Laplace pressure gradient across the Plateau border. This happens until the inertio-capillary time, $T_c \sim 10^{-2}$ s. Note that this can be simply realised by observing eq. (2) where, the source term (in parenthesis) is minimised, damped by the Trouton viscosity. The damped oscillations appearing in fig. 4 are a manifestation of this process.

From this time onward, the plug-flow is minimised and the surface tension gradient relaxation process comes into play through eq. (3). We thus have a period of transition from a plug-flow to a development of a Poiseuille-flow across the thin film. The duration of this transition phase depends non-monotonically on the mixture concentration. Once the Poiseuille-flow is set up, we have the main stage of film-thinning which follows a power law dependence. Focusing on the film thinning law, $h_{min} \sim t^n$, we observe a value of $n = -0.66 \pm 0.06$ throughout the range of mixture concentration, c_0. In this context, experimental film thinning laws are scarcely reported, but an exponent of $n = -2/3$ has been experimentally found at least in the case of thin-film evolution influenced by sparse surfactants [1]. Our model, being governed by surfactant-like effect predicts close to this scaling, as shown in Fig. 4. Earlier models [4, 15, 16], for a similar geometry involving Plateau borders, relevant to thin films in foams, predict a scaling exponent of $n = -1/2$ when a Poiseuille flow with immobile interfaces is considered. On the other hand, when a mobile interface is considered with a plug flow in the bulk, the film thins very rapidly with an exponent of $n = -2$ which predicts the dynamics in thin films of pure liquids; as also reported in Ref. [18]. The model presented in this letter does not rely on such assumptions and predicts the film evolution consistent with the experiments of Ref. [1]. To the best of our knowledge, this is the first time the exponent of $n = -2/3$ for the film thinning law is predicted for pinching of thin-films involving Plateau borders.

Finally, we present our model predictions of film lifetimes in fig. 4 (inset) as a function of mixture concentrations. It has been reported earlier experimentally that the lifetimes of foams and surface bubbles of binary

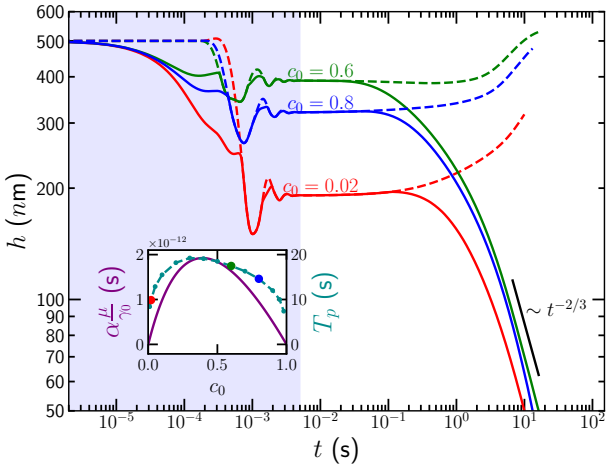

FIG. 4. Film evolution at the pinch region, h_{min} (solid curves) and at the center, h_c (dashed curves) for octane-toluene mixture. The shaded region corresponds to the initial fast process of film tension equilibration. Subsequent relaxation of surface tension leads to the film thinning law: $h_{min} \sim t^{-2/3}$. The molar surface, $\sigma = 2.5 \times 10^5$ m^2/mol. [Inset] Model predictions of pinching times of film T_p [teal] compared to $\alpha\mu/\gamma_0$ [purple] for octane-toluene mixture. Color coded circles correspond to c_0 values of the main plot.

mixture (translated to a length-scale) correlate with the Gibbs modulus parameter, α [12]. Our model predicts a similar correlation and is thus able to account for experimental observations despite the geometrical differences. As a perspective of the current study, we point out that the estimated times are highly sensitive to aspect ratio $(\mathcal{H}/\mathcal{L})$ and length scales $(\mathcal{L}, h_i, R_b)$. Further, an estimation of time-scale for the marginal pinching process requires a careful estimation of the dimensions of pinch region, which correlate to the physicochemical parameters of the binary mixture.

To summarize, we develop a model describing dynamics of marginal pinching in surfactant-like systems. The model comprising of coupled evolution equations for film thickness, mean velocity and surface tension describes the interplay between capillary drainage and a concomitant Marangoni flow. The parabolic component of the resulting Poiseuille flow is subtly included in the leading order derivation and additionally appears as a second gradient of surface tension. In the current letter, we obtain variations of pinching times for binary mixtures in a canonical geometry of a Scheludko cell which are in agreement with experiments. Further, the predicted dynamics agree well with qualitative behaviors observed in recent experiments of surface bubbles with sparse-surfactant effects, for example, the *marginal regeneration* reported in contaminated water [1] and the tension equilibration process reported in salt solutions [17]. The model presented here is versatile in nature, providing a recipe to model other foamy systems governed by linear surface tension variation relevant for dilute surfactant-like effects.

[1] H. Lhuissier and E. Villermaux, Bursting bubble aerosols, Journal of Fluid Mechanics **696**, 5 (2012).

[2] B. Petkova, S. Tcholakova, M. Chenkova, K. Golemanov, N. Denkov, D. Thorley, and S. Stoyanov, Foamability of aqueous solutions: Role of surfactant type and concentration, Advances in Colloid and Interface Science **276**, 102084 (2020).

[3] M. Pasquet, F. Boulogne, J. Sant-Anna, F. Restagno, and E. Rio, The impact of physical-chemistry on film thinning in surface bubbles, Soft Matter **18**, 4536 (2022), num Pages: 7 Place: Cambridge Publisher: Royal Soc Chemistry Web of Science ID: WOS:000807087400001.

[4] E. Klaseboer, J. P. Chevaillier, C. Gourdon, and O. Masbernat, Film drainage between colliding drops at constant approach velocity: experiments and modeling, Journal of colloid and interface science **229**, 274 (2000).

[5] J. Zawala, J. Miguet, P. Rastogi, O. Atasi, M. Borkowski, B. Scheid, and G. G. Fuller, Coalescence of surface bubbles: The crucial role of motion-induced dynamic adsorption layer, Advances in Colloid and Interface Science **317**, 102916 (2023).

[6] B. Petkova, S. Tcholakova, and N. Denkov, Foamability of surfactant solutions: Interplay between adsorption and hydrodynamic conditions, Colloids and Surfaces A: Physicochemical and Engineering Aspects **626**, 127009 (2021).

[7] V. Chandran Suja, A. Kar, W. Cates, S. M. Remmert, P. D. Savage, and G. G. Fuller, Evaporation-induced foam stabilization in lubricating oils, Proc. Natl. Acad. Sci. U.S.A. **115**, 7919 (2018).

[8] L. Lombardi, S. Roig-Sanchez, A. Bapat, and J. M. Frostad, Nonaqueous foam stabilization mechanisms in the presence of volatile solvents, Journal of Colloid and Interface Science **648**, 46 (2023).

[9] S. Ross and G. Nishioka, Foaminess of binary and ternary solutions, J. Phys. Chem. **79**, 1561 (1975).

[10] R. Pugh, Foaming, foam films, antifoaming and defoaming, Advances in colloid and interface science **64**, 67 (1996).

[11] H.-P. Tran, M. Arangalage, L. Jørgensen, N. Passade-Boupat, F. Lequeux, and L. Talini, Understanding frothing of liquid mixtures: A surfactantlike effect at the origin of enhanced liquid film lifetimes, Physical Review Letters **125**, 178002 (2020).

[12] H.-P. Tran, N. Passade-Boupat, F. Lequeux, and L. Talini, Mechanisms ruling the lifetimes of films of liquid mixtures, Journal of Fluid Mechanics **944**, A55 (2022).

[13] M. V. D. Tempel, J. Lucassen, and E. H. Lucassen-Reynders, Application of Surface Thermodynamics to Gibbs Elasticity, J. Phys. Chem. **69**, 1798 (1965).

[14] C. Trégouët and I. Cantat, Instability of the one-dimensional thickness profile at the edge of a horizontal foam film and its Plateau border, Phys. Rev. Fluids **6**, 114005 (2021).

[15] A. Aradian, E. Raphael, and P.-G. De Gennes, "marginal pinching" in soap films, Europhysics Letters **55**, 834 (2001).

[16] M. S. Shah, C. R. Kleijn, M. T. Kreutzer, and V. Van Steijn, Influence of initial film radius and film thickness on the rupture of foam films, Physical Review Fluids **6**, 013603 (2021).

[17] B. Liu, R. Manica, Q. Liu, Z. Xu, E. Klaseboer, and Q. Yang, Nanoscale transport during liquid film thinning inhibits bubble coalescing behavior in electrolyte solutions, Physical Review Letters **131**, 104003 (2023).

[18] C. Breward and P. Howell, The drainage of a foam lamella, Journal of Fluid Mechanics **458**, 379 (2002).

[19] See supplemental material for detailed theoretical derivation, data on numerical simulations and an animation of a simulation.

[20] J. Eggers and T. F. Dupont, Drop formation in a one-dimensional approximation of the navier–stokes equation, Journal of fluid mechanics **262**, 205 (1994).

[21] A. Choudhury, V. K. Paidi, S. K. Kalpathy, and H. N. Dixit, Enhanced stability of free viscous films due to surface viscosity, Physics of Fluids **32** (2020).

[22] J. A. V. Butler, The thermodynamics of the surfaces of solutions, Proceedings of the Royal Society of London. Series A, Containing Papers of a Mathematical and Physical Character **135**, 348 (1932), publisher: Royal Society.

[23] L. Duchemin and J. Eggers, The explicit-implicit-null method: Removing the numerical instability of pdes, J. Comput. Phys. **263**, 37 (2014).

[24] G. d. Debrégeas, P.-G. De Gennes, and F. Brochard-Wyart, The life and death of" bare" viscous bubbles, Science **279**, 1704 (1998).